

Catalytic and Structural Role of a Conserved Active Site Histidine in Berberine Bridge Enzyme

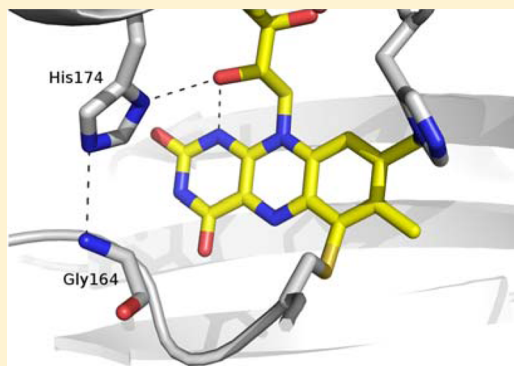
Silvia Wallner,[†] Andreas Winkler,^{†,§} Sabrina Riedl,^{†,||} Corinna Dully,[†] Stefanie Horvath,[†] Karl Gruber,^{*,‡} and Peter Macheroux^{*,†}

[†]Institute of Biochemistry, Graz University of Technology, Petersgasse 12/2, A-8010 Graz, Austria

[‡]Institute of Molecular Biosciences, University of Graz, Humboldtstraße 50/3, A-8010 Graz, Austria

S Supporting Information

ABSTRACT: Berberine bridge enzyme (BBE) is a paradigm for the class of bicovalently flavinylated oxidases, which catalyzes the oxidative cyclization of (*S*)-reticuline to (*S*)-scoulerine. His174 was identified as an important active site residue because of its role in the stabilization of the reduced state of the flavin cofactor. It is also strictly conserved in the family of BBE-like oxidases. Here, we present a detailed biochemical and structural characterization of a His174Ala variant supporting its importance during catalysis and for the structural organization of the active site. Substantial changes in all kinetic parameters and a decrease in midpoint potential were observed for the BBE His174Ala variant protein. Moreover, the crystal structure of the BBE His174Ala variant showed significant structural rearrangements compared to wild-type enzyme. On the basis of our findings, we propose that His174 is part of a hydrogen bonding network that stabilizes the negative charge at the N1–C2=O locus via interaction with the hydroxyl group at C2' of the ribityl side chain of the flavin cofactor. Hence, replacement of this residue with alanine reduces the stabilizing effect for the transiently formed negative charge and results in drastically decreased kinetic parameters as well as a lower midpoint redox potential.



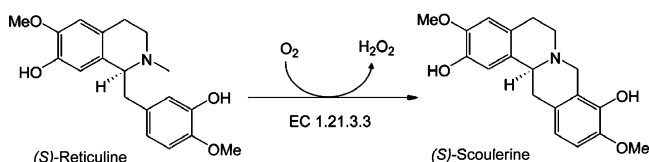
Enzymes with bicovalently linked flavin cofactors have repeatedly been demonstrated to catalyze challenging chemical reactions in both eukaryotic and prokaryotic systems.^{1–10} Today, the number of enzymes known to possess both covalent cysteinyl and histidinylation of the flavin is increasing, and extensive research in identifying new members of this class of flavoproteins has been conducted. However, despite these ongoing studies, the mechanism of bicovalent tethering of the flavin cofactor and the influence of conserved amino acid residues on flavin reactivity are not fully understood and require further investigation. Here we present a mutagenic analysis of berberine bridge enzyme [BBE, (*S*)-reticuline oxidase, EC 1.21.3.3], which addresses the role of His174 in flavin reactivity and bicovalent cofactor linkage.

BBE is a well-characterized flavin-dependent oxidase, which catalyzes the unique oxidative cyclization of the *N*-methyl moiety of (*S*)-reticuline into the berberine bridge atom of (*S*)-scoulerine (Scheme 1).^{1,11} It was shown before that BBE

belongs to a recently discovered protein family with bicovalent cofactor binding.¹ A structure-based mutagenic analysis led to a deeper understanding of the role of bicovalent flavinylation for catalysis and to the proposal of a concerted mechanism for BBE.¹² It was demonstrated that bicovalent flavinylation shifts the redox potential of the cofactor to a remarkably high value of 132 mV and hence facilitates the oxidative ring closure in (*S*)-reticuline, yielding (*S*)-scoulerine as the product.¹³ Replacement of either residue forming the covalent linkages to the cofactor (Cys166 or His104) with Ala resulted in a decrease in the midpoint potential of the flavin and in lower rates of substrate turnover.^{2,13}

Recent studies of various oxidases revealed that catalysis requires stabilization of the transiently formed negative charge at the N1–C2=O locus of the flavin cofactor.^{14,15} Thus, positively charged amino acids such as lysine^{16–20} or arginine²¹ are frequently positioned in the vicinity of the N1 position of the isoalloxazine ring to stabilize the uptake of the negative charge in the flavin ring system. Moreover, a histidine residue^{22–24} or a helix dipole^{14,25–27} can supply the positive charge for stabilization. In BBE, no such functionality can be found near the N1–C2=O locus, indicating that stabilization of the negative charge is achieved by a different mechanism.

Scheme 1



Received: March 31, 2012

Revised: June 12, 2012

Published: July 3, 2012

Although this positive charge is missing in BBE, a tyrosine and a histidine residue are positioned near the N1–C2=O locus and can interact directly or via the C2' hydroxyl group of the ribityl side chain of the flavin. Interestingly, the respective histidine residue (His174) is conserved among related bicovalently flavinylated proteins with oxidase activity, whereas no strict conservation is found for the corresponding tyrosine residue. Hence, here we addressed the role of His174 for stabilizing the negative charge during the course of catalysis.

The mechanism of covalent flavinylation has been studied for representative proteins with monocovalently tethered flavins.^{28–31} In all cases, flavinylation was reported to occur autocatalytically, and for most investigated proteins, similar mechanisms for covalent flavin coupling at C8 α were suggested.¹⁴ The proposed mechanism starts with abstraction of a proton from the C8 methyl group of the flavin with subsequent stabilization of the negative charge at the N1–C2=O locus of the isoalloxazine ring.¹⁴ Again, some examples have shown that this stabilization can be attributed to a positive amino acid residue such as a lysine in monomeric sarcosine oxidase¹⁸ or an arginine in *p*-cresol methylhydroxylase²¹ and vanillyl-alcohol oxidase.¹⁴ Until now, no bicovalently flavinylated protein has been investigated with regard to mechanistic aspects of bicovalent flavin attachment. Previous mutagenesis studies showed that both covalent linkages seem to form independently of each other, because both histidinylated and cysteinylated single-variant proteins could be expressed and isolated.^{2,3,13,14,32} However, amino acid residues involved in the process of covalent flavin attachment were not addressed. Because of the strong conservation of the His174 residue situated in the proximity of the N1–C2=O locus of the isoalloxazine ring system, we wanted to address its role for bicovalent flavinylation.

Thus, in this study, a BBE variant in which the conserved histidine residue His174 was replaced with alanine was created and the influence of this amino acid residue on spectral and kinetic parameters as well as on the midpoint potential of the flavin cofactor was determined. Moreover, the crystal structure of the His174Ala variant protein was determined to a resolution of 2.65 Å (PDB entry 4EC3). Here we demonstrate that His174 plays a role in stabilizing the negative charge in the isoalloxazine ring system during catalysis, because the respective variant protein features a reduced midpoint potential of the cofactor and significantly decreased overall enzyme efficiency. Also, covalent flavinylation seems to be affected by the removal of His174 because artificially reduced protein reversibly breaks and re-forms 6-S-cysteinylated in an oxygen-dependent manner.

■ EXPERIMENTAL PROCEDURES

Reagents. All chemicals were purchased from Sigma-Aldrich and were of the highest quality available. The QuikChange XL kit for site-directed mutagenesis was from Stratagene, and oligonucleotide primers were ordered from VBC-Biotech. (*S*)-Reticuline was obtained from the natural product collection at the Donald Danforth Plant Science Center (St. Louis, MO).

Site-Directed Mutagenesis. Mutagenesis was performed following the instructions of the QuikChange XL kit for site-directed mutagenesis (Stratagene) using expression vector pPICZ α BBE-ER as described in ref 1 as a template for the polymerase chain reaction. Replacement of His174 with Ala was accomplished by using 5'-CGTTGGTACTGGGGGT-

GCTATTAGTGGT-3' as the sense primer and the complementary antisense primer. The underlined nucleotides represent the mutated codon. Introduction of the desired mutation was verified by plasmid sequencing.

Transformation, Expression, and Protein Purification.

The newly generated expression plasmid pPICZ α BBE H174A was transformed into *Pichia pastoris* KM71H using electroporation. Integration of the expression cassettes into the *Pichia* genome was verified using colony polymerase chain reaction. Applicable expression strains were identified on a small scale in 300 mL shake flasks with 50 mL of buffered minimal dextrose medium. Induction was started with 0.1% methanol with consecutive methanol additions as described in ref 33. Large scale expression of the BBE variant protein was conducted in a BBI CT5-2 fermenter (Sartorius). Fermentation was performed following the *Pichia* Fermentation Process Guidelines from Invitrogen with a modified basal salt medium.³⁴ After a 96 h methanol induction, the fermentation was stopped and purification was performed as described previously.^{1,34} Expression of the correct variant protein was verified by matrix-assisted laser desorption ionization time-of-flight mass spectrometry as described previously.¹

Steady-State Kinetic Analysis. Steady-state turnover rates were determined by following the conversion of (*S*)-reticuline to (*S*)-scoulerine by high-performance liquid chromatography analysis of the reaction mixture as described previously.¹

Transient Kinetics. Reductive half-reactions were analyzed with a stopped-flow device (SF-61DX2, Hi-Tech) in an anaerobic atmosphere of approximately 0.8 ppm oxygen in a glovebox from Belle Technology. All samples were rendered oxygen-free by being flushed with nitrogen and subsequent incubation in the glovebox. Changes in flavin absorbance were followed using a PM-61s photomultiplier or a KinetaScanT diode array detector (MG-6560). Apparent rate constants for the reductive half-reaction were determined at six different substrate concentrations from 30 to 300 μ M (*S*)-reticuline with a protein concentration of 15 μ M in 150 mM NaCl and 50 mM Tris-HCl (pH 9.0 and 37 °C). Fitting of the obtained transients at 446 nm was performed with SpecFit 32 (Spectrum Software Associates) using a function of two exponentials.

Rates for the oxidative half-reaction were determined by mixing air-saturated buffer (21% oxygen) with a substrate-reduced enzyme solution. Reduction of the flavin cofactor was performed with substoichiometric amounts of (*S*)-reticuline to prevent lag phases in the reoxidation process.

Anaerobic Photoreduction. Anaerobic photoreduction was conducted as described in ref 35. The reaction mixture consisted of 1 mM EDTA, 1 μ M 5-deazariboflavin, and a 15 μ M enzyme solution in 150 mM NaCl and 50 mM Tris-HCl at different pH values (5.0–9.0). Prior to photoreduction, the reaction mixtures were rendered anaerobic by repeated cycles of evacuation and flushing with nitrogen in a special glass cuvette. Photoillumination was conducted with a conventional slide projector. All spectra were recorded with a Specord 205 spectrophotometer (Analytic Jena) at 25 °C; 7.5 M urea in 50 mM Tris-HCl (pH 8.0) or acetonitrile was used for the denaturation of completely reduced protein samples. For denaturation, the anaerobic samples were mixed in equal amounts with denaturation reagent (urea or acetonitrile) and were kept at 60 °C for 45 min. Afterward, spectra of the denatured protein samples were recorded.

Redox Potential Determination. Redox potentials were determined using the dye-equilibration method with the

xanthine/xanthine oxidase electron delivering system as described by Massey.³⁶ All experiments were performed in 50 mM potassium phosphate buffer (pH 7.0) at 25 °C containing benzyl viologen (5 μ M) as a mediator, 250 μ M xanthine, and xanthine oxidase in catalytic amounts (approximately 1 nM). To maintain anaerobic conditions, all experiments were conducted with a stopped-flow device (SF-61DX2, Hi-Tech) positioned in a glovebox from Belle Technology. Spectra were recorded with a KinetaScanT diode array detector (MG-6560). Toluylene blue ($E_M = 115$ mV), thionine acetate ($E_M = 64$ mV), toluidine blue ($E_M = 34$ mV), and indigotrisulfonic acid potassium salt ($E_M = -81$ mV) were used as dyes for redox potential determination. The potentials were calculated from plots of $\log([\text{ox}]/[\text{red}])$ of the respective BBE variant protein versus $\log([\text{ox}]/[\text{red}])$ of the dye according to the method of Minnaert.³⁷

Crystallization and Data Collection. Crystallization of the BBE His174Ala variant was essentially performed as described previously for BBE variants His104Ala and Cys166Ala.¹² Briefly, crushed crystals of wild-type BBE grown using the sitting drop vapor diffusion method¹² were used for microseeding crystallization setups of the BBE His174Ala variant. These were prepared by mixing 0.8 μ L of protein at 120 mg/mL with 1.2 μ L of reservoir solution [0.2 M MgCl₂ and 30% (w/v) polyethylene glycol 4000 in 0.1 M Tris-HCl (pH 8.5)] and equilibrated for 16 h prior to being seeded. Monoclinic crystals appeared after 1 week and continued to grow for 3 weeks prior to reaching the final dimensions. Substrate-soaked crystals were then obtained by a 5 min incubation in the presence of 20 mM (*S*)-reticuline in the reservoir solution prior to being flash-frozen in liquid nitrogen.

A data set for a substrate-soaked His174Ala crystal was collected at beamline X11, DESY (Hamburg, Germany). Processing of the data was performed using XDS,³⁸ and because of isomorphism with monoclinic wild-type BBE crystals (PDB entry 3D2H), the structure could be determined by rigid body fitting using PHENIX.³⁹ The obtained model was further refined using the same software starting with simulated annealing followed by several rounds of maximum likelihood least-squares refinement of models modified using the graphics program Coot⁴⁰ employing σ_A -weighted $2F_o - F_c$ and $F_o - F_c$ electron density maps. A summary of data collection, processing, and refinement statistics is presented in Table S1 of the Supporting Information. R_{free} values⁴¹ were computed from a randomly chosen 5% of reflections not used throughout the refinement. (*S*)-Reticuline was excluded from the initial refinement process and inserted only in later rounds when clear electron density was visible.

RESULTS

General Properties. BBE His174Ala was expressed in *P. pastoris* KM71H cells using the fermentation protocol established for wild-type BBE.¹ The protein could be detected in the fermentation supernatant in amounts similar to the amount of wild-type BBE, and purification was performed using a two-step purification protocol with consecutive hydrophobic interaction and gel filtration chromatography. To test for covalent attachment of the FAD cofactor, protein samples were precipitated with 13% (w/v) trichloroacetic acid, and no free flavin could be detected in the supernatant after centrifugation. Thus, it was assumed that in BBE His174Ala the flavin cofactor is bound in a covalent manner. This finding was later confirmed by elucidation of the three-dimensional X-ray structure of the

variant protein. The observed electron density demonstrates a clear bicovalent linkage of the FAD to His104 and Cys166 at positions 8 α and 6, respectively (Figure 1).

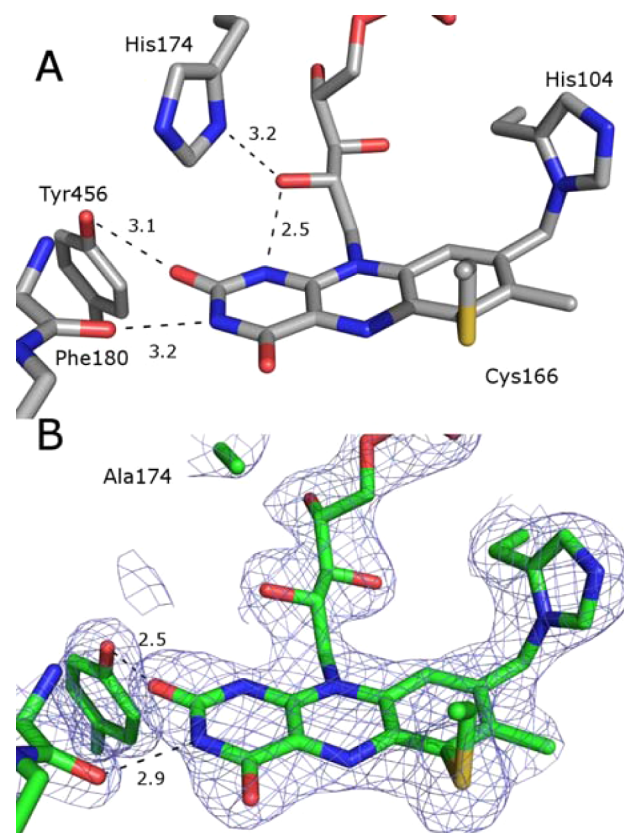


Figure 1. (A) Amino acids in the proximity of the N1–C2=O region of the isoalloxazine ring system of wild-type BBE. (B) For comparison, the same region is shown for the His174Ala variant protein structure, showing the sideways movement of the flavin ring as indicated by the strengthened hydrogen bond to Tyr456 and the Phe180 main chain carbonyl. The electron density shown in panel B represents the $2F_o - F_c$ map contoured at 1.5σ . Distances for hydrogen bonds are given in angstroms.

Spectral Properties. UV–visible absorbance spectra were recorded for native and denatured variant protein and are shown in Figure 2. The spectral characteristics of His174Ala reflect the covalent flavinylation as observed for wild-type BBE.¹ The spectrum after denaturation shows only one absorption maximum at ~ 440 nm and thus indicates a modification of the flavin in its C6 position.^{13,42}

Photoreduction. Photoreduction was performed in the presence of EDTA and 5-deazariboflavin by exposing the anaerobic sample to light. His174Ala showed a different reduction pattern compared to that of wild-type BBE, and spectra recorded during the reduction of this variant are shown in Figure 3. Light illumination of the His174Ala variant leads to a marginal formation of a red anionic semiquinone, which was already shown for both wild-type BBE and the Cys166Ala variant.¹³ After the apparent complete reduction of the His174Ala variant, a nonisosteric hypsochromic shift of the absorption maximum to ~ 357 nm was observed, which was not detected in wild-type BBE (Figure S1 of the Supporting Information). However, more significant differences between wild-type BBE and the His174Ala variant were observed upon

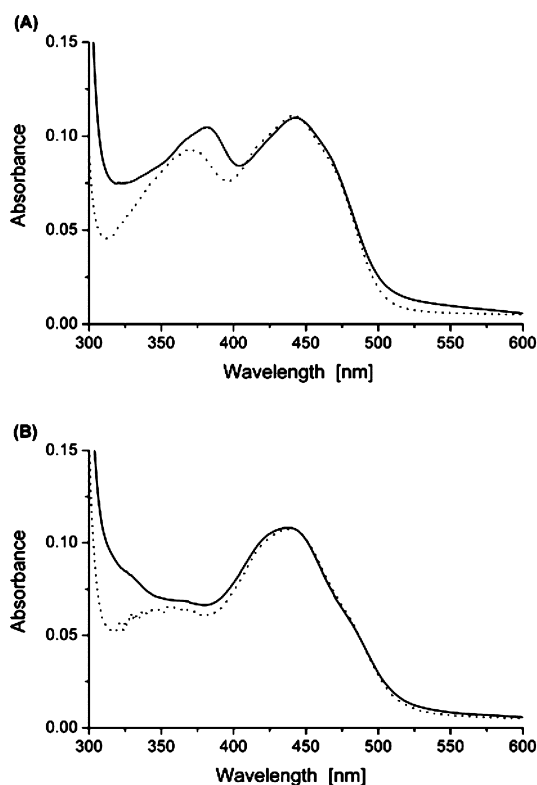


Figure 2. Absorption spectra of the His174Ala variant in comparison to the wild-type enzyme. Absorption spectra of the native enzymes (A) and the enzymes after heat denaturation (B). Solid lines represent data for the wild-type enzyme in its native and denatured form. Dashed lines represent data for the His174Ala variant. All spectra are normalized to a protein concentration of $\sim 10 \mu\text{M}$.

reoxidation of the flavin cofactor after complete photoreduction. Reoxidation of wild-type BBE resulted in an absorption spectrum with a long wavelength absorbance between 550 and 900 nm, which is indicative of the generation of 6-thio FAD.¹ However, reoxidation of the His174Ala variant protein resulted in an absorption spectrum with characteristics of the Cys166Ala variant, and no 6-thio FAD was observed.¹³ In the case of the His174Ala variant, the resulting spectrum of the reoxidized FAD cofactor showed a broad maximum ranging from 350 to 370 nm, which suggests a cleavage of the 6-S-cysteinyl bond. Interestingly, when the compound is exposed to oxygen, this spectrum slowly loses its broad maximum, and after some hours, virtually the same spectrum as at the beginning of the experiment was obtained. Thus, it is suggested that the covalent cysteinyl bond is reversibly cleaved upon complete photoreduction and that reoxidation of the cofactor induces an autocatalytic process for re-forming the covalent linkage. To test this hypothesis, the completely reduced species was denatured by the addition of urea from a side arm of the anaerobic cuvette. The absorption spectra of the fully reduced and subsequently denatured His174Ala variant are shown in Figure 4. Strikingly, the resulting spectrum has spectral properties similar to those of the Cys166Ala variant by exhibiting two absorption maxima at ~ 350 and 450 nm .⁴² Again, this is indicative of a cleavage of the 6-S-cysteinyl linkage in His174Ala, which seems to occur in the last phase of photoreduction. Thus, it appears that the covalent flavinylation is affected by the removal of His174 because the wild-type and

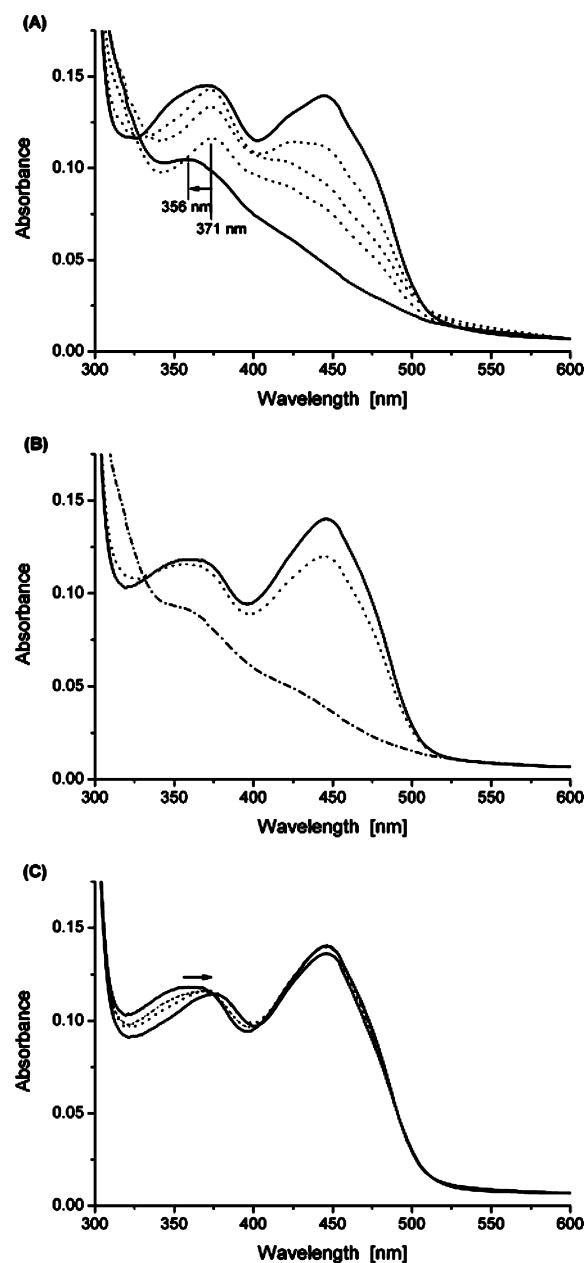


Figure 3. Anaerobic photoreduction and reoxidation of BBE His174Ala. (A) Selected spectra of the complete photoreduction. Solid lines represent the spectrum prior to illumination and the spectrum of the fully reduced flavin cofactor. Dotted lines are selected spectra recorded during the course of photoreduction. The hypsochromic shift in the maximum of the fully reduced species to 350 nm is indicated by a black arrow. (B) Selected spectra recorded upon admission of oxygen: (---) spectrum of the fully reduced flavin cofactor after photoillumination, (...) spectrum after a 5 s exposure to oxygen, and (—) characteristic spectrum of BBE His174Ala after reoxidation. (C) Slow regeneration of the initial absorption spectrum. Solid lines are spectra of the flavin cofactor 5 min and 5 h after the admission of oxygen. Dashed lines show spectral changes that indicate a slow regeneration of the flavin cofactor.

variant enzymes exhibit different behavior upon photoirradiation.

Redox Potential Determination. To improve our understanding of the influence of His174 on the covalent flavinylation and kinetic properties of the His174Ala variant, the redox potential of the FAD cofactor was determined. A

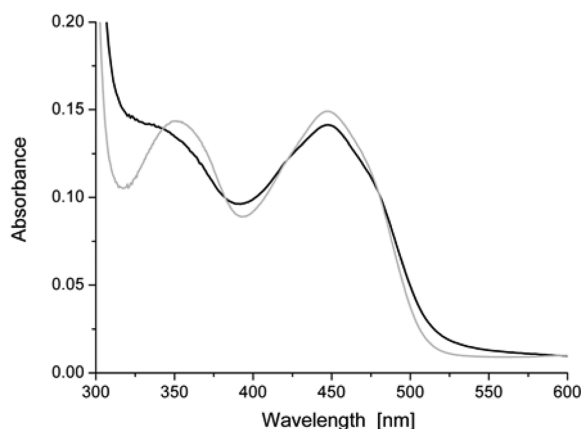


Figure 4. Absorption spectrum of completely reduced and consecutively denatured His174Ala. The black line is the spectrum of BBE His174Ala denatured in its completely reduced form, whereas the gray line is the absorption spectrum of denatured Cys166Ala.

xanthine/xanthine oxidase system in the presence of suitable redox indicators was used, and a plot of $\log(\text{BBE}_{\text{ox}}/\text{BBE}_{\text{red}})$ versus $\log(\text{dye}_{\text{ox}}/\text{dye}_{\text{red}})$ as described by Minnaert³⁷ allowed the estimation of the respective redox potential. Interestingly, the His174Ala variant protein features a midpoint potential of 44 mV, which rather resembles the potentials of the Cys166Ala and His104Ala variants with only one covalent cofactor linkage. The crystal structure of BBE His174Ala, however, shows clear electron density for an α -histidyl and a 6-S-cysteinyl bond and hence did not suggest a decreased midpoint potential, because of incomplete formation of the bicovalent linkage.

Kinetic Characterization. We determined the kinetic properties of BBE His174Ala to address the role of His174 for catalysis. High-performance liquid chromatography was used to analyze the reaction mixture after various time points of (S)-reticuline conversion as reported for wild-type BBE.¹ Table 1 shows a compilation of kinetic parameters determined for the His174Ala variant protein, wild-type BBE, and the variant proteins with one missing covalent linkage (Cys166Ala and His104Ala).

Substantial changes in all kinetic parameters were observed for BBE His174Ala. A k_{cat} value of $0.07 \pm 0.01 \text{ s}^{-1}$ was determined, which accounts for an ~ 120 -fold decrease in catalytic activity compared to that of the wild-type enzyme ($k_{\text{cat}} = 8.0 \pm 0.2 \text{ s}^{-1}$). Thus, BBE His174Ala is less active than the monocovalently linked Cys166Ala and His104Ala variant proteins.^{2,13} Addition of exogenous imidazole to the reaction mixture buffer did not rescue the activity of the His174Ala variant. In the presence of 100 mM imidazole, the k_{cat} value of His174Ala was determined to be $0.134 \pm 0.038 \text{ s}^{-1}$, which implies a very small effect on k_{cat} compared to the value of $0.07 \pm 0.01 \text{ s}^{-1}$ in the absence of exogenous imidazole.

For the BBE His174Ala variant, an 8-fold increase in the K_{d} value was observed compared to that of the wild-type enzyme (K_{d} values of 68 ± 30 and $8.7 \pm 0.8 \mu\text{M}$ for BBE His174Ala and wild type, respectively), which implies that replacement of His174 affects substrate binding. To address the influence of the introduced amino acid exchange on specific reaction steps, reductive and oxidative half-reactions of (S)-reticuline conversion were assessed for the His174Ala variant. Again, all experiments were performed under identical reaction conditions as described for wild-type BBE.¹ Interestingly, the His174Ala variant protein exhibited a very pronounced effect on the reductive half-reaction. For the His174Ala variant, a limiting reductive rate of $0.08 \pm 0.01 \text{ s}^{-1}$ was determined, which is an ~ 1300 -fold decrease in k_{red} compared to that of the wild type ($k_{\text{red}} = 103 \pm 4 \text{ s}^{-1}$).

The oxidative rate was also influenced by the His to Ala replacement, yielding a k_{ox} of $(7.0 \pm 0.3) \times 10^3 \text{ M}^{-1} \text{ s}^{-1}$ compared to a value of $(0.5 \pm 0.1) \times 10^5 \text{ M}^{-1} \text{ s}^{-1}$ for the wild-type enzyme.¹²

It was shown before that for the wild-type enzyme the oxidative step is the rate-limiting step in substrate turnover.¹³ However, the kinetic parameters of BBE His174Ala suggest that the substantially decreased reductive rate can be regarded as the rate-limiting step in the enzymatic turnover of the variant protein. Similar properties were observed for BBE Glu417Gln, where the catalytic glutamate residue was replaced with glutamine. For Glu417Gln, a limiting reductive rate of $0.067 \pm 0.007 \text{ s}^{-1}$ was observed,¹² which is similar to the rate determined for BBE His174Ala.

Structural Characterization. To rationalize the observed significant changes in the rate constants for both reductive and oxidative reaction steps, we determined the crystal structure of BBE His174Ala. Because of the pronounced reduction in the reductive rate, the crystal was soaked with (S)-reticuline to allow a better characterization of the mode of substrate binding. However, only slow-growing monoclinic crystals of the His174Ala variant could be obtained, which because of their comparatively small size did not diffract as well as in the case of the wild-type protein or the His104Ala and Cys166Ala variants described previously.^{2,12} With respect to the substrate-soaked wild-type crystals, however, the resolution of 2.65 Å is slightly better than the resolution of 2.8 Å obtained previously with wild-type BBE.

Initial electron density maps confirmed the presence of the bicovalent cofactor attachment and replacement of His174 with Ala (Figure 1 B). While the overall structural change compared to both the monoclinic and tetragonal crystal forms is relatively small (root-mean-square deviations for C α atoms of 0.28 and 0.39 for PDB entries 3D2D and 3D2J¹²), there are some significant structural rearrangements extending from the site of the amino acid substitution to the substrate binding site. As shown in Figure 5, removal of the histidine side chain leads to a peptide flip of the neighboring Ala163 residue with its carbonyl

Table 1. Summary of the Kinetic Parameters^a

BBE	$k_{\text{red}} (\text{s}^{-1})$	$k_{\text{ox}} (\text{M}^{-1} \text{s}^{-1})$	$k_{\text{cat}} (\text{s}^{-1})$	$E_0 (\text{mV})$	$K_{\text{d}} (\mu\text{M})$
H174A	0.08 ± 0.01	$(7.0 \pm 0.3) \times 10^3$	0.07 ± 0.01	44 ± 3	68 ± 30
wild type	103 ± 4	$(0.5 \pm 0.1) \times 10^5$	8.0 ± 0.2	132 ± 4	8.7 ± 0.8
C166A	0.28 ± 0.02	$(1.0 \pm 0.1) \times 10^5$	0.48 ± 0.05	53 ± 2	17 ± 3
H104A	3.4 ± 0.3	$(0.8 \pm 0.1) \times 10^5$	0.54 ± 0.02	28 ± 4	4 ± 2

^aKinetic data for wild-type BBE, C166A, and H104A proteins were taken from refs 1 and 2.

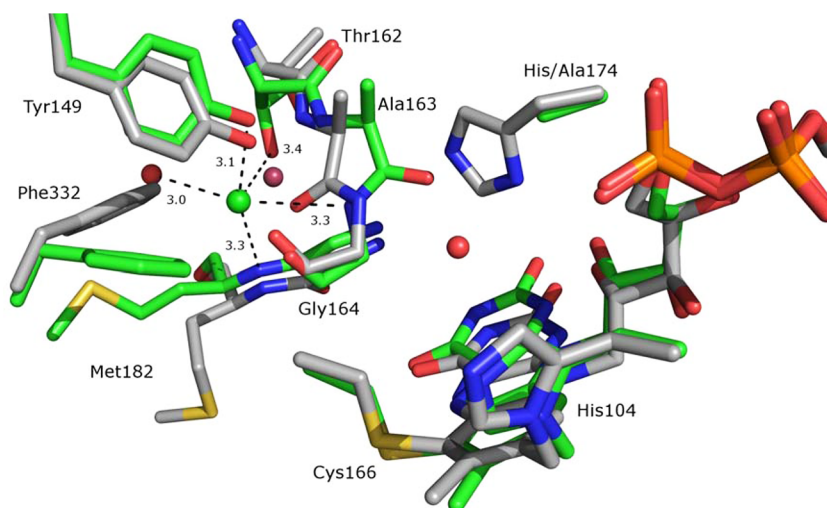


Figure 5. Structural changes due to His174Ala substitution observed in the proximity of the isoalloxazine ring system. Wild-type carbon atoms are colored gray, and the corresponding elements of the His174Ala structure are colored green. Because of the missing imidazole ring of His174, a flipped peptide bond is observed between Ala163 and Gly164. The corresponding amide proton then provides one ligand for a newly formed chloride binding site. Distances for the partial octahedral coordination of the anion are given in angstroms. Water molecules colored red belong to His174Ala, and the one colored violet belongs to the wild-type protein. The bound chloride ion is colored green.

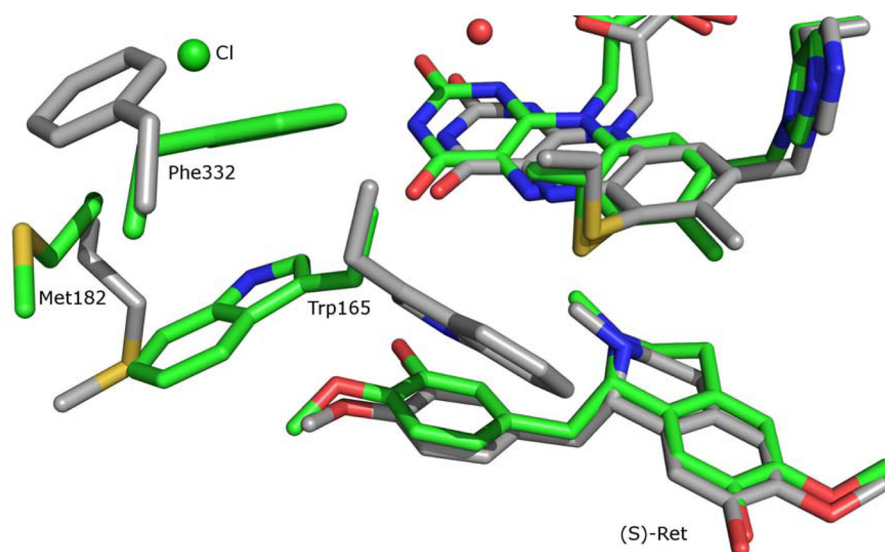


Figure 6. Additional structural changes due to altered amino acid side chains involved in the formation of the chloride ion coordination shell. With Phe332 as a starting point, these changes extend via Met182 all the way to the active site amino acid Trp165, which is in direct contact with the substrate (*S*)-reticuline. Wild-type carbon amino acids are colored gray, and the corresponding amino acids of the His174Ala variant are colored green.

oxygen now forming a hydrogen bond to an ordered water molecule present on the *re* side of the isoalloxazine ring close C4a, which had not been observed in the substrate-soaked monoclinic wild-type structure.¹² Interestingly, also the amide proton of the same peptide bond interacts with a ligand not seen in any of the previously described structures. The chloride ion positioned into the electron density for this ligand is supported by its refined *B* factor, which is close to that of the surrounding water molecules, and its well-defined octahedral coordination with average distances of 3.2 Å to its hydrogen bond donors (Figure 5). As a consequence of the newly formed chloride binding site, the side chain of Phe332 is repositioned and via Met182 also induces rearrangements of Trp165, which is an important residue in the substrate binding site of BBE (Figure 6). Moreover, also the isoalloxazine of the flavin

cofactor itself is shifted by ~1 Å into the back of the substrate binding pocket because of the missing hydrogen bond between His174 and the C2' hydroxyl group of the ribityl chain. This in turn opens space for a different rotamer of Phe351, which renders the whole active site entrance loop more ordered than the wild-type structures. With all these changes occurring in the active site of the protein, it is also interesting to note that the mode of (*S*)-reticuline binding itself is only marginally affected by the His174Ala mutation. However, the backward movement of the isoalloxazine ring system is partially followed by the substrate increasing the hydrogen bond distance to the catalytic base Glu417 from 2.8 Å in the wild-type structure¹² to 3.2 Å. Another important feature of the electron density shown in Figure 1 is its intactness with respect to the isoalloxazine ring system, although the crystal was incubated for 4 weeks under

conditions identical to those of wild-type BBE crystallized in the same crystal form. For the latter protein, degradation of the flavin to the 4a-spirohydantoin was already observed after 5 days (PDB entry 3D2D),¹² suggesting a reduced reactivity of the flavin cofactor with respect to potential degradation pathways in the His174Ala variant.

DISCUSSION

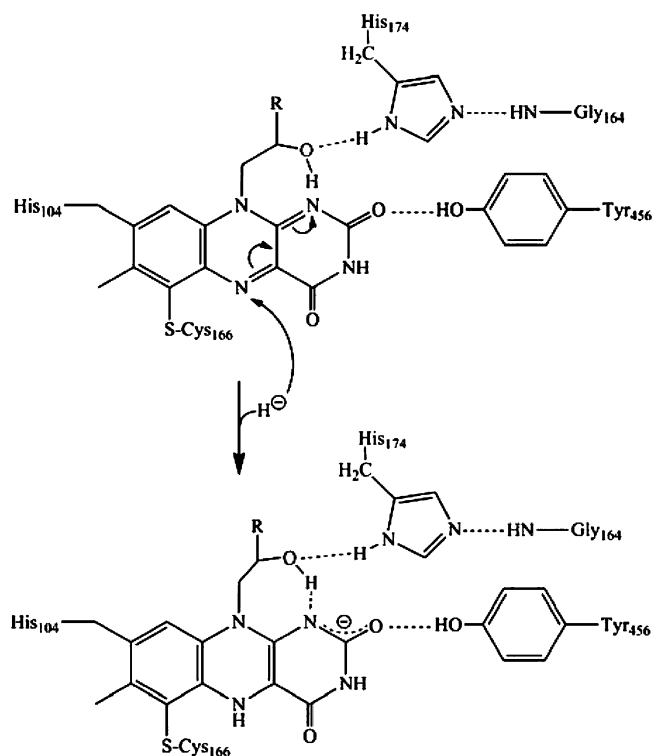
The major objective of this study was to investigate the role of His174, a conserved active site amino acid among bivalent flavoproteins, for substrate turnover and bivalent flavinylation of BBE. Sequence alignments of all known bivalently linked flavoproteins showed that all bivalent oxidases feature this histidine residue that interacts with the C2' hydroxyl group of the ribityl side chain of the flavin cofactor (Figure 1A). Interestingly, GilR from *Streptomyces* sp. and most pollen allergens from different grasses possess a leucine or an asparagine residue instead of the conserved histidine (see Figure S2 of the Supporting Information). Recently, GilR was identified as the first bivalently linked dehydrogenase,⁴ and for most pollen allergens, no catalytic function had been demonstrated until now.

However, initial studies of Phl p 4 from timothy grass also showed the dehydrogenase activity of the enzyme (W. Keller and D. Zafred, University of Graz, personal communication). These findings suggest that the conserved histidine residue is especially important for oxidases but not for dehydrogenases within this family of bivalent flavoenzymes.

A pronounced influence of the His174Ala replacement was observed for all kinetic parameters. An ~120-fold decrease in catalytic activity compared to that of the wild-type enzyme was determined for the His174Ala variant protein. This influence is much stronger than that of the monovalently linked BBE variants (Cys166Ala and His104Ala) and is in the range of that of the Glu417Gln variant protein, where the catalytic glutamate residue was exchanged.¹² Strikingly, the same effect was obtained for the reductive rate of BBE His174Ala. A drastic 1300-fold decrease in k_{red} was determined compared to that of the wild-type enzyme. Hence, the reduced k_{red} and k_{cat} values of the His174Ala variant suggest that His174 is required for efficient catalysis. It is obvious from the wild-type crystal structure that His174 cannot directly interact with the flavin isoalloxazine ring; however, it is involved in a hydrogen bonding network by interacting with the C2' hydroxyl group of the ribityl side chain of the flavin that again interacts with the N1–C2=O locus of the isoalloxazine ring system. Hence, this hydrogen bond network might stabilize the intermediate negative charge during substrate turnover (Scheme 2). This lack of stabilization of the reduced form of the cofactor could also explain the decreased redox potential of the His174Ala variant protein. Although this variant features a bivalent cofactor linkage, its redox potential (44 ± 3 mV) is lowered compared to that of the wild-type enzyme (132 ± 4 mV) but is in the range of the monovalent Cys166Ala and His104Ala variant proteins (53 ± 2 and 28 ± 4 mV, respectively).

Moreover, the substantially decreased rate of substrate turnover is attributed not only to the lack of stabilization of the negatively charged intermediate but also to structural alterations. In the crystal structure of the His174Ala mutant protein, the flavin cofactor and the substrate (*S*)-reticuline are slightly shifted in the active site, leading to an increased distance between the catalytically essential Glu417 and the 3'-hydroxyl residue of the substrate. In a previous study, we have

Scheme 2



shown that Glu417 initiates substrate oxidation by deprotonation of the 3'-hydroxyl residue of (*S*)-reticuline.¹² This deprotonation increases the nucleophilicity of the C2' atom that then attacks the *N*-methyl group of the substrate, resulting in methylene bridge formation and the concomitant transfer of a hydride to the flavin cofactor. Hence, an increased hydrogen bonding distance between Glu417 and the C3' hydroxyl residue could hamper proton abstraction and hence slow the initiation of the concerted reaction. Besides this strong influence on k_{cat} and k_{red} , we also observed a 7-fold decrease in the oxidative rate when histidine 174 was replaced with alanine. Interestingly, His174Ala was the first BBE variant protein with a significant effect on the rate of cofactor reoxidation. In the crystal structure of the His174Ala variant protein, a peptide flip of Ala163 that forms a hydrogen bond to a structured water molecule in the substrate-soaked crystal is observed. This water molecule possibly influences reoxidation of the reduced cofactor by interfering with the site for dioxygen binding.⁴³ For flavin-dependent oxidases, a glycine or a proline residue was suggested to be required for providing enough space for allowing dioxygen access to the isoalloxazine ring.⁴³ Gly164, which forms a hydrogen bond to His174, was identified as the respective amino acid residue in BBE.⁴³ Removal of His174 results in a new orientation of Gly164, which now might prevent oxygen from accessing the flavin cofactor.

The hydrogen bonding interaction between Gly164 and His174 also suggests that His174 is unlikely to exist as a positively charged imidazolium and is present as imidazole in BBE (Figure 1 and Scheme 2).

Moreover, interesting observations were made upon photo-reduction of the BBE His174Ala variant protein. When the wild-type enzyme is completely reduced by photoirradiation, 6-thio FAD is formed, which can effectively be stabilized by histidine 174.¹ In case of the His174Ala variant, no 6-thio FAD was observed, which might be attributed to a lack of

stabilization of this modified flavin. In the His174Ala variant, full reduction of the flavin cofactor resulted in the cleavage of the C6–sulfur bond, i.e., the cysteinyl linkage (Figure 4). Here, the resulting spectrum rather resembled that of the denatured Cys166Ala variant with only one covalent linkage.

In conclusion, our results have shown that His174 is an essential active site residue in BBE, which participates in the stabilization of the reduced form of the flavin by maintaining a hydrogen bond network via the ribityl C2' hydroxyl residue. Moreover, His174 engages in a hydrogen bond interaction with the main chain amide group of Gly164, which is apparently beneficial for the proper alignment of other residues involved in the enzymatic reaction, such as Trp165. Hence, the replacement of His174 destabilizes the reduced state of FAD by disrupting the hydrogen bond network, leading to a less favorable redox potential of the cofactor and a rearrangement of other amino acid residues in and near the active site of the enzyme.

■ ASSOCIATED CONTENT

📄 Supporting Information

Data statistics of X-ray crystallography, figures that supplement the Results, and a sequence alignment of bicovalent flavoproteins. This material is available free of charge via the Internet at <http://pubs.acs.org>.

■ AUTHOR INFORMATION

Corresponding Author

*K.G.: Institute of Molecular Biosciences, University of Graz, Humboldtstraße 50/3, A-8010 Graz, Austria; telephone, +43-316-380 5483; fax, +43-316-380 9897; e-mail, karl.gruber@uni-graz.at. P.M.: Institute of Biochemistry, Graz University of Technology, Petersgasse 12/2, A-8010 Graz, Austria; telephone, +43-316-873 6450; fax, +43-316-873 6952; e-mail, peter.macheroux@tugraz.at.

Present Addresses

§Department for Biomolecular Mechanisms, Max Planck Institute for Medical Research, Jahnstraße 29, D-69120 Heidelberg, Germany.

||Institute of Biophysics and Nanosystems Research, Austrian Academy of Sciences, Schmiedlstraße 6, A-8042 Graz, Austria.

Author Contributions

S.W. and A.W. contributed equally to this work.

Notes

The authors declare no competing financial interest.

■ ABBREVIATIONS

BBE, berberine bridge enzyme; FAD, flavin adenine dinucleotide; GilR, pregilvocarcin V dehydrogenase; PDB, Protein Data Bank; XDS, X-ray detector software.

■ REFERENCES

- (1) Winkler, A., Hartner, F., Kutchan, T. M., Glieder, A., and Macheroux, P. (2006) Biochemical evidence that berberine bridge enzyme belongs to a novel family of flavoproteins containing a bi-covalently attached FAD cofactor. *J. Biol. Chem.* **281**, 21276–21285.
- (2) Winkler, A., Motz, K., Riedl, S., Puhl, M., Macheroux, P., and Gruber, K. (2009) Structural and mechanistic studies reveal the functional role of bicovalent flavinylation in berberine bridge enzyme. *J. Biol. Chem.* **284**, 19993–20001.
- (3) Heuts, D. P. H. M., Winter, R. T., Damsma, G. E., Janssen, D. B., and Fraaije, M. W. (2008) The role of double covalent flavin binding

in chito-oligosaccharide oxidase from *Fusarium graminearum*. *Biochem. J.* **413**, 175–183.

(4) Kharel, M. K., Pahari, P., Lian, H., and Rohr, J. (2009) GilR, an unusual lactone-forming enzyme involved in gilvocarcin biosynthesis. *ChemBioChem* **10**, 1305–1308.

(5) Mo, X., Huang, H., Ma, J., Wang, Z., Wang, B., Zhang, S., Zhang, C., and Ju, J. (2011) Characterization of TrdL as a 10-hydroxy dehydrogenase and generation of new analogues from a tirandamycin biosynthetic pathway. *Org. Lett.* **13**, 2212–2215.

(6) Carlson, J. C., Li, S., Gunatilleke, S. S., Anzai, Y., Burr, D. A., Podust, L. M., and Sherman, D. H. (2011) Tirandamycin biosynthesis is mediated by co-dependent oxidative enzymes. *Nat. Chem.* **3**, 628–633.

(7) Rand, T., Qvist, K. B., Walter, C. P., and Poulsen, C. H. (2006) Characterization of the flavin association in hexose oxidase from *Chondrus crispus*. *FEBS J.* **273**, 2693–2703.

(8) Huang, C. H., Lai, W. L., Lee, M. H., Chen, C. J., Vasella, A., Tsai, Y. C., and Liaw, S. H. (2005) Crystal structure of glucooligosaccharide oxidase from *Acremonium strictum*: A novel flavinylation of 6-S-cysteinyl, 8 α -N1-histidyl FAD. *J. Biol. Chem.* **280**, 38831–38838.

(9) Alexeev, I., Sultana, A., Mäntylä, P., Niemi, J., and Schneider, G. (2007) Aclacinomycin oxidoreductase (AknOx) from the biosynthetic pathway of the antibiotic aclacinomycin is an unusual flavoenzyme with a dual active site. *Proc. Natl. Acad. Sci. U.S.A.* **104**, 6170–6175.

(10) Sosio, M., Stinchi, S., Beltrametti, F., Lazzarini, A., and Donadio, S. (2003) The gene cluster for the biosynthesis of the glycopeptide antibiotic A40926 by *Nonomuraea* species. *Chem. Biol.* **10**, 541–549.

(11) Dittrich, H., and Kutchan, T. M. (1991) Molecular cloning, expression, and induction of berberine bridge enzyme, an enzyme essential to the formation of benzophenanthridine alkaloids in the response of plants to pathogenic attack. *Proc. Natl. Acad. Sci. U.S.A.* **88**, 9969–9973.

(12) Winkler, A., Łyskowski, A., Riedl, S., Puhl, M., Kutchan, T. M., Macheroux, P., and Gruber, K. (2008) A concerted mechanism for berberine bridge enzyme. *Nat. Chem. Biol.* **4**, 739–741.

(13) Winkler, A., Kutchan, T. M., and Macheroux, P. (2007) 6-S-Cysteinylated bi-covalently attached FAD in berberine bridge enzyme tunes the redox potential for optimal activity. *J. Biol. Chem.* **282**, 24437–24443.

(14) Heuts, D. P. H. M., Scrutton, N. S., McIntire, W. S., and Fraaije, M. W. (2009) What's in a covalent bond?: On the role and formation of covalently bound flavin cofactors. *FEBS J.* **276**, 3405–3427.

(15) Fraaije, M. W., and Mattevi, A. (2000) Flavoenzymes: Diverse catalysts with recurrent features. *Trends Biochem. Sci.* **25**, 126–132.

(16) Wagner, M. A., Trickey, P., Che, Z. W., Mathews, F. S., and Jorns, M. S. (2000) Monomeric sarcosine oxidase: I. Flavin reactivity and active site binding determinants. *Biochemistry* **39**, 8813–8824.

(17) Lindqvist, Y., and Branden, C. I. (1989) The active site of spinach glycolate oxidase. *J. Biol. Chem.* **264**, 3624–3628.

(18) Trickey, P., Wagner, M. A., Jorns, M. S., and Mathews, F. S. (1999) Monomeric sarcosine oxidase: Structure of a covalently flavinylated amine oxidizing enzyme. *Structure* **7**, 331–345.

(19) Muh, U., Massey, V., and Williams, C. H., Jr. (1994) Lactate monooxygenase. I. Expression of the mycobacterial gene in *Escherichia coli* and site-directed mutagenesis of lysine 266. *J. Biol. Chem.* **269**, 7982–7988.

(20) Xia, Z. X., and Mathews, F. S. (1990) Molecular structure of flavocytochrome b₂ at 2.4 Å resolution. *J. Mol. Biol.* **212**, 837–863.

(21) Efimov, I., Cronin, C. N., Bergmann, D. J., Kuusk, V., and McIntire, W. S. (2004) Insight into covalent flavinylation and catalysis from redox, spectral, and kinetic analyses of the R474K mutant of the flavoprotein subunit of *p*-cresol methylhydroxylase. *Biochemistry* **43**, 6138–6148.

(22) Ghanem, M., and Gadda, G. (2006) Effects of reversing the protein positive charge in the proximity of the flavin N(1) locus of choline oxidase. *Biochemistry* **45**, 3437–3447.

(23) Hecht, H. J., Kalisz, H. M., Hendle, J., Schmid, R. D., and Schomburg, D. (1993) Crystal structure of glucose oxidase from *Aspergillus niger* refined at 2.3 Å resolution. *J. Mol. Biol.* **229**, 153–172.

- (24) Wohlfahrt, G., Witt, S., Hendle, J., Schomburg, D., Kalisz, H. M., and Hecht, H. J. (1999) 1.8 and 1.9 Å resolution structures of the *Penicillium amagasakiense* and *Aspergillus niger* glucose oxidases as a basis for modelling substrate complexes. *Acta Crystallogr. D55*, 969–977.
- (25) Vrielink, A., Lloyd, L. F., and Blow, D. M. (1991) Crystal structure of cholesterol oxidase from *Brevibacterium sterolicum* refined at 1.8 Å resolution. *J. Mol. Biol.* 219, 533–554.
- (26) Hallberg, B. M., Henriksson, G., Pettersson, G., and Divne, C. (2002) Crystal structure of the flavoprotein domain of the extracellular flavocytochrome cellobiose dehydrogenase. *J. Mol. Biol.* 315, 421–434.
- (27) Mattevi, A., Vanoni, M. A., Todone, F., Rizzi, M., Teplyakov, A., Coda, A., Bolognesi, M., and Curti, B. (1996) Crystal structure of D-amino acid oxidase: A case of active site mirror-image convergent evolution with flavocytochrome b₂. *Proc. Natl. Acad. Sci. U.S.A.* 93, 7496–7501.
- (28) Jin, J., Mazon, H., Van Den Heuvel, R. H. T., Heck, A. J., Janssen, D. B., and Fraaije, M. W. (2008) Covalent flavinylation of vanillyl-alcohol oxidase is an autocatalytic process. *FEBS J.* 275, 5191–5200.
- (29) Kim, J., Fullert, J. H., Kuusk, V., Cunane, L., Chen, Z. W., Mathews, F. S., and McIntire, W. S. (1995) The cytochrome subunit is necessary for covalent FAD attachment to the flavoprotein subunit of *p*-cresol methylhydroxylase. *J. Biol. Chem.* 270, 31202–31209.
- (30) Hassan-Abdallah, A., Bruckner, R. C., Zhao, G., and Jorns, M. S. (2005) Biosynthesis of covalently bound flavin: isolation and *in vitro* flavinylation of the monomeric sarcosine oxidase apoprotein. *Biochemistry* 44, 6452–6462.
- (31) Brandsch, R., and Bichler, V. (1991) Autoflavinylation of apo6-hydroxy-D-nicotine oxidase. *J. Biol. Chem.* 266, 19056–19062.
- (32) Huang, C. H., Winkler, A., Chen, C. L., Lai, W. L., Tsai, Y. C., Macheroux, P., and Liaw, S. H. (2008) Functional roles of the 6-S-cysteinylyl, 8 α -N1-histidyl FAD in glucooligosaccharide oxidase from *Acremonium strictum*. *J. Biol. Chem.* 283, 30990–30996.
- (33) Weis, R., Luiten, R., Skranc, W., Schwab, H., Wubbolts, M., and Glieder, A. (2004) Reliable high-throughput screening with *Pichia pastoris* by limiting yeast cell death phenomena. *FEMS Yeast Res.* 5, 179–189.
- (34) Schrittwieser, J. H., Resch, V., Wallner, S., Lienhart, W. D., Sattler, J. H., Resch, J., Macheroux, P., and Kroutil, W. (2011) Biocatalytic organic synthesis of optically pure (*S*)-p-coulerine and berbine and benzyloquinoline alkaloids. *J. Org. Chem.* 76, 6703–6714.
- (35) Massey, V., and Hemmerich, P. (1978) Photoreduction of flavoproteins and other biological compounds catalyzed by deazaflavins. *Biochemistry* 17, 9–17.
- (36) Massey, V. (1991) in *Flavins and Flavoproteins* (Curti, B., Zanetti, G., and Ronchi, S., Eds.) pp 59–66, Walter de Gruyter, Como, Italy.
- (37) Minnaert, K. (1965) Measurement of the equilibrium constant of the reaction between cytochrome c and cytochrome a. *Biochim. Biophys. Acta* 110, 42–56.
- (38) Kabsch, W. (1993) Automatic processing of rotation diffraction data from crystals of initially unknown dymmetry and cell constants. *J. Appl. Crystallogr.* 26, 795–800.
- (39) Adams, P. D., Grosse-Kunstleve, R. W., Hung, L., Ioerger, T. R., McCoy, A. J., Moriarty, N. W., Read, R. J., Sacchettini, J. C., Sauter, N. K., and Terwilliger, T. C. (2002) PHENIX: Building new software for automated crystallographic structure determination. *Acta Crystallogr. D58*, 1948–1954.
- (40) Emsley, P., and Cowtan, K. (2004) Coot: Model-building tools for molecular graphics. *Acta Crystallogr. D60*, 2126–2132.
- (41) Kleywegt, G. J., and Brunger, A. T. (1996) Checking your imagination: Applications of the free R value. *Structure* 4, 897–904.
- (42) Singer, T. P., and Edmondson, D. E. (1980) Structure, Properties, and Determination of Covalently Bound Flavins. *Methods Enzymol.* 66, 353–264.
- (43) Leferink, N. G. H., Fraaije, M. W., Joosten, H.-J., Schaap, P. J., Mattevi, A., and van Berkel, W. J. H. (2009) Identification of a Gatekeeper Residue That Prevents Dehydrogenases from Acting as Oxidases. *J. Biol. Chem.* 284, 4392–4397.